Optical Oxygen Sensing Materials Based on the Room-temperature Phosphorescence Intensity Quenching of Immobilized Erythrosin B

Marta Elena Diaz-Garcia, Rosario Pereiro-García and Nieves Velasco-García

Department of Physical and Analytical Chemistry, Faculty of Chemistry, C/Julian Claveria, 8, University of Oviedo, 33006 Oviedo, Spain

The organic dye, Erythrosin B, exhibits strong room-temperature phosphorescence (RTP) when adsorbed on non-ionic resins or when encapsulated in silicone rubber films. In this paper, oxygen transducers based on the RTP intensity quenching of the immobilized dye (on Amberlite XAD-2 or embedded in silicone) have been optically and analytically characterized using continuous and gas-phase flow injection systems. The sensing phases proved to have good photochemical stability. Detection limits of 0.0005% of oxygen in dry argon were found and s_r values of around 0.3% (at 0.02% oxygen level) were achieved. Typical response times were less than 2 s for full signal change and no hysteresis in the response was observed.

Keywords: *Room-temperature phosphorescence; oxygen sensing; Erythrosin B; flow injection; quenching*

Introduction

Monitoring concentrations of molecular oxygen is of great importance in medical care, *e.g.*, in critical care, assisting in anaesthesiology, in pulmonary examinations, *etc.*[1,2] The development of new techniques and methods to measure molecular oxygen has attracted continuous effort over the last decade. The inherent advantages of optical sensors for oxygen, based on the quenching of the luminescence of appropriate indicators (such as lack of oxygen consumption and inertness against sample flow rates or stirring[3]) have encouraged research in that area. The possibility of being coupled to long fibre optics provides a means for remote-sensing of oxygen.

Polycyclic aromatic hydrocarbons[4,5] and transition metal complexes (especially those with platinum metals[6–9]) are the most commonly used fluorescent indicators for oxygen sensing. The application of the quenching of room-temperature phosphorescence (RTP) by oxygen was first described more than fifty years ago: the detection of traces of oxygen produced in photosynthetic processes and the measurement of the diffusion coefficient of oxygen in acrylics was performed using organic dyes such as, trypaflavine, acridine, safranine or hematoporphyrin adsorbed on silica gel or aluminium oxide.[3,10] Unfortunately, most dyes are photolabile, and traces of water interfere strongly.[3,10,11] Recently, the use of RTP metal chelates like Pd^{II}- [or Pt^{II}-] coprophorphyrins in solution, or immobilized on polymer films,[12,13] the platinum dimer tetrakis(pyrophosphito) diplatinate(II) embedded in silicone,[14] and 8-hydroxy-7-iodo-5-quinolinesulfonic acid (ferron) chelates of some transition metals retained on anion-exchange resin beads[15] have been proposed for oxygen sensing. In principle, RTP quenching based oxygen sensors offer several advantages over fluorescent ones. Most of these advantages arise from the longer excited-state lifetimes of phosphorescent reagents, which give rise to high-quenching effectiveness by oxygen, and to low-noise analytical signals.[16,17] Moreover, the RTP backgrounds from conventional solid supports, where the luminophor is usually immobilized (*e.g.*, organic resins or common polymer films), are negligible. These properties makes the search and characterization of new RTP oxygen sensing phases a field of great research interest.

In this paper, an RTP phase, based on immobilized Erythrosin B, is proposed for the optical sensing of oxygen. Non-ionic resin beads of Amberlite XAD-2 and silicone membranes have been studied as dye solid supports. Optimization and optical characterization of the sensing phases is described, the effect of water as a quencher of the RTP emission and the sensor's analytical performance for gaseous mixtures is evaluated using continuous flow and flow injection (FI) systems. In this last case, gas samples are transiently introduced into the flow system with a gas exponential dilution manifold.[18]

Experimental

Materials

The selected reagent, Erythrosin B, was provided by Carlo Erba (Milan, Italy) and was used without further purification. The non-ionic polymeric adsorbent Amberlite XAD-2 (20–60 mesh) (Sigma, St. Louis, MO, USA) was used as the dye solid support. The Amberlite impurities were removed by washing the resin first with ethanol, in order to displace air from the pores of the resin and to remove residual monomers and solvents, and then with de-ionized water. The washed resins were dried at 120 °C for 3 h. Lower mesh particle sizes (200–400 mesh) were prepared in the laboratory by applying crushing and sieving procedures to the commercial resin.

Silicone rubber (Silicex, Silicona Hispania SA) used was a clear rubber without a filler, such as silica. Air, argon, oxygen, carbon dioxide, nitrogen and helium, all with purity higher than 99.995%, were purchased from Sociedad Española del Oxígeno. All other chemicals were of analytical-reagent grade.

Preparation of the Oxygen-sensing Beads and the Sensing Films

Impregnated resins (active phases) with different concentrations of adsorbed reagent were prepared by immersing 0.1 g of the dry support in 4 ml of Erythrosin B solution for 10 h, with intermittent stirring. Erythrosin B solutions of different concentrations were prepared by dissolving the appropriate amount of reagent in 100 ml of liquid solution containing 90 ml of ethanol and 10 ml of 0.1 mol l^{-1} acetic acid–sodium acetate buffer solution, at pH 6. To evaluate the exact amount of reagent fixed per gram of support, the dye not adsorbed in the immobilization process was quantified by measuring the fluorescence of the remaining solution. The phosphorescent

sensing beads were washed with de-ionized water, dried at 40 °C, and kept dry until use.

The oxygen sensing films were prepared by either one of the following methods: (*i*) dispensing the sensing beads [Erythrosin B immobilized on small size Amberlite XAD-2 resin particles (200–400 mesh)] in silicone rubber (following a similar procedure to that described previously[15]), (*ii*) mixing the dye (50 μl of 10^{-3} mol l^{-1} solutions of Erythrosin B in ethanol) thoroughly with 0.068 g of silicone rubber, before casting the silicone to make the film.

Instrumentation

All RTP data were collected with a Perkin-Elmer LS 5 luminescence spectrometer, which employs a xenon-pulsed (10 μs half-width, 50 Hz) excitation source and is equipped with a Perkin-Elmer 3600 data station. The delay time was normally set at 0.04 ms and the gate time was 2 ms for RTP measurements. The triplet lifetimes were obtained by using the 'Obey-Decay' application program. To apply this program it is necesssary to set six delay time values. The delay times selected for our studies were: 0.04, 0.06, 0.08, 0.10 0.12 and 0.15 ms.

For some experiments, 20–60 mesh active beads were directly packed on a conventional Hellma (Mullheim, Germany) flow-cell (Model 176.52) as previously described.[15] In the case of experiments with sensing films, the membrane was positioned on a laboratory-made front-surface flow-through cell with an inner volume of about 150 μl. The flow cell, fabricated from Perspex, has a rectangular quartz window to which the sensing membrane is adhered. The design and dimensions of this flow cell, which fitted in the spectrometer sample compartment, are given elsewhere.[15]

The phosphorescence intensities were monitored at 625 nm and/or at 700 nm, with excitation (in all cases) at 550 nm, and all the measurements were made at room temperature (20 ± 2 °C) and 101.325 KPa (1 atm).

Gas Flow Optosensing Manifolds and Procedures of Operation

Fig. 1 illustrates the two optosensing systems for continuous and transient (*i.e.*, discrete) introduction of gas mixtures. For the continuous mode [Fig. 1(*a*)], a steady environment with various concentrations of oxygen was maintained in the flow cell by varying the relative flow rates of compressed oxygen (or pure air, 21.0% O_2) and argon. Two mass flow controllers were used to measure the relative flow rates of oxygen and argon. The total gas flow rate was kept constant at 200 ml min^{-1}. Back diffusion processes in the mixing tee limit the use of this system to air–argon ratios higher than 2% of oxygen.

A transient sample introduction manifold, which can be considered as a gas-phase FI system, was used to lead to the sensor levels of oxygen lower than 2%. In this case, the gas sample is introduced into the gas flow system using an exponential dilution chamber.[18] This device consists of a 140 ml glass vessel, as shown in Fig. 1(*b*), containing a magnetic stirrer to allow gas homogeneity. Samples (air or pure oxygen) are introduced into the vessel (filled with argon) with a Hamilton gas-tight syringe (Teknokroma, Barcelona, Spain), through a septum. The exponential dilution chamber is provided with a three-way stopcock which allows the carrier gas (argon at a flow rate of 200 ml min^{-1}) to pass directly to the sensor or to go through the vessel dragging the sample to the sensing phase. In this second step, an initial concentration, c_o, in the vessel is diluted continuously according to[18]

$$c(t) = c_o \exp(-Ft/V)$$

where $c(t)$ is the concentration at time t; F is the flow rate of the argon carrier gas; t is the time spent after the stopcock was turned, and V is the volume of the vessel. Therefore, this sample introduction system gives rise to the formation of sample plugs which reach the detector with an exponential decay concentration profile.

Results and Discussion

Optical Characteristics of Erythrosin B in Solution and Immobilized on Amberlite XAD-2

Erythrosin B is a tetraiodo-substituted xanthene dye. Solutions of Erythrosin B in ethanol or in aqueous buffers 0.1 mol l^{-1} acetic acid–sodium acetate at pHs ranging from 4.5 to 6.5 proved to be fluorescent but no RTP emissions were observed either in the presence of oxygen or in deoxygenated

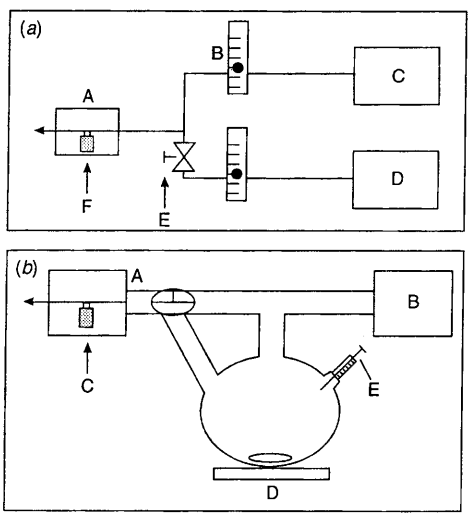

Fig. 1 (*a*) Optosensing manifold for continuous gas-flow system for oxygen sensing. A, spectrofluorimeter; B, mass flow controller; C, argon cylinder; D, air cylinder; E, needle valve; and F, sensor. (*b*) Manifold for gas-flow injection oxygen sensing. A, spectrofluorimeter; B, argon cylinder; C, sensor; D, magnetic stirrer; and E, septum for gasesous sample injection.

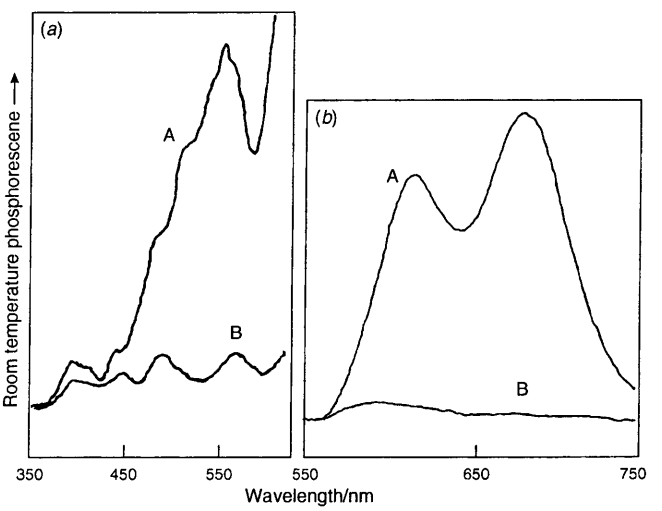

Fig. 2 Room temperature phosphorescence spectra of the immobilized dye in Amberlite XAD-2 (20–60 mesh) in A, argon and in B, air environments. Sensing beads with 6.2×10^{-7} mol Erythrosin B per gram of XAD-2. (*a*) excitation spectrum and (*b*) phosphorescence spectrum.

media (in this latter case, solutions were chemically deoxygenated with 1×10^{-2} mol l^{-1} sodium sulfite).[19] The excitation and the RTP spectra of Erythrosin B immobilized on XAD-2 are recorded in Fig. 2. A delay time of 0.04 ms was used for these experiments to ensure that any fluorescence from the dye and the support had ceased. As can be seen, the excitation spectra obtained in the absence of oxygen (argon environments) has an intense maximum at about 550 nm, while two maxima, at 625 nm and 700 nm, respectively, were observed for the RTP emission spectra. The RTP emission intensity is severely quenched in the presence of air. As can be seen, air environments decrease completely the intensity of both RTP emission bands. The more intense maximum at 700 nm, which has also larger single–triplet splitting, was chosen for most subsequent experiments.

Selection of the Concentration of Erythrosin B Immobilized on the Resin Beads

Sensing beads 20–60 mesh with different concentrations of adsorbed dye, prepared following the procedure described in the Experimental Section, were packed in a conventional flow cell.[15] The RTP emission intensity in the absence of oxygen (I_{Ar}) and the ratios I_{Ar}/A_{air} (I_{air} corresponds to the RTP intensity in air) were measured. Results are shown in Fig. 3. As can be seen, the concentration which provided higher I_{Ar} intensities was 3.6×10^{-7} mol of Erythrosin B per gram of XAD-2. This concentration of reagent adsorbed on the sensing beads was obtained using a 1×10^{-5} mol l^{-1} solution of Erythrosin B in the preparation of the sensing phase. However, insignificant differences in the I_{Ar}/I_{air} ratios were observed for the five types of sensing beads assayed. The resin with higher RTP emission intensities was selected for further work.

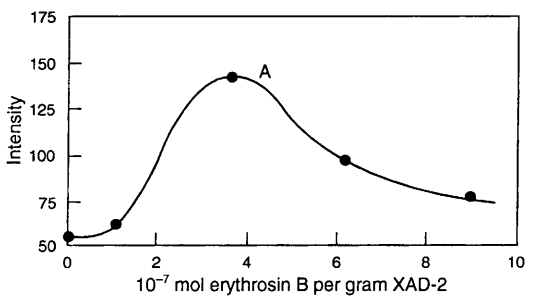

Fig. 3 Effect of the concentration of Erythrosin B adsorbed onto Amberlite XAD-2 on RTP intensities in the absence of oxygen. A = 3.6×10^{-7} mol erythrosin B per gram XAD-2.

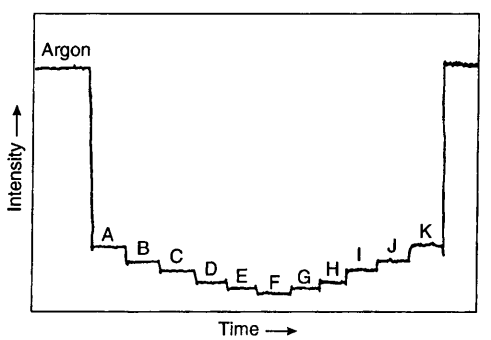

Fig. 4 Dynamic response of the luminescence intensity of the sensing beads to increasing and decreasing oxygen concentrations. A, 1.4; B, 1.7; C, 3.0; D, 4.2; E, 5.7; F, 7.6; G, 5.7; H, 4.2; I, 3.0; J, 1.7; and K, 1.4% O_2.

Performance of the Selected Sensing Beads

It was found that the sensing beads, when packed directly into the flow cell, respond reversibly to the presence of oxygen in gaseous mixtures and that the response time for full signal change was less than 2 s. Also, as shown in Fig. 4, no hysteresis effects were observed. Moreover, the proposed sensing beads proved to be photochemically stable in the presence of both oxygen and argon. No substantial decrease in the RTP intensity of this active phase was observed after more than 30 h of continuous illumination.

The influence of the temperature on the Stern–Volmer responses for oxygen was tested. As expected, the higher the temperature, the poorer the sensitivity. For example, an increase from 20 to 50 °C worsened the oxygen detection limit by 45%. A temperature of 20 °C was maintained for the subsequent experiments.

The effect of some foreign gases on the photochemical characteristics of the proposed sensor was evaluated. The selectivity study was focused on the major air components, nitrogen and carbon dioxide (the latter very important in pulmonary examinations). Light helium was also investigated in order to preclude a possible role of argon as the external heavy atom of the RTP emission of the immobilized dye. Results confirmed that none of these gases produce any effect in the determination of oxygen. In fact, it was observed that even if nitrogen, carbon dioxide or helium were used as carrier gases instead of argon, no influence in the I_o/I ratios for oxygen was observed (the study was performed with 5% oxygen levels).

Analytical performance characteristics of the proposed sensing beads were evaluated. As was stated under Experimental, standard calibration graphs for oxygen concentrations lower than 2% were prepared using an exponential dilution manifold, which gives rise to FI-like signals [see Fig. 5(*a*)]. Calibration graphs, for Stern–Volmer intensity quenching plots are shown in Fig. 5(*b*). The lack of linearity of the plot could be attributed to inhomogeneities of the

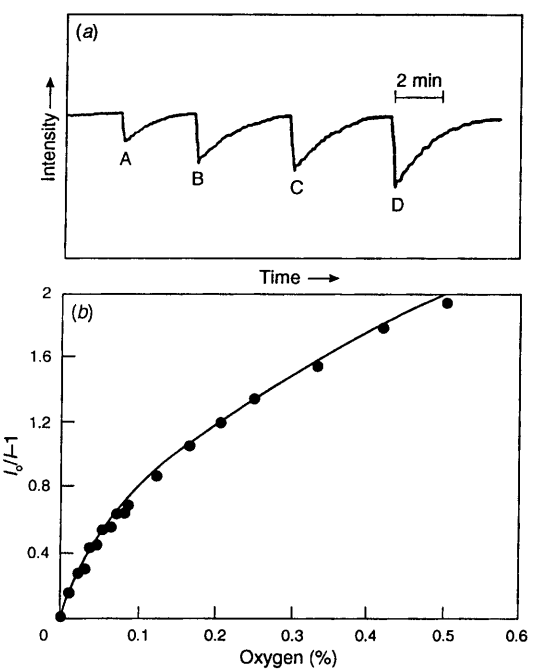

Fig. 5 Typical response of the sensing beads toward oxygen in gas mixtures introduced in a FI-like system. (*a*) Response–time curves. A, 0.008; B, 0.02; C, 0.025; and D, 0.034% O_2. (*b*) Stern–Volmer calibration plot.

environment where the luminophor is immobilized.[7] For the chosen sensing phase, mathematical data treatment showed a linear correlation of $I_o/I - 1$ *versus* the square root of the concentration of oxygen, being the linear regressions higher than 0.9995. The detection limit, estimated as the concentration of oxygen which produced an analytical signal equal to 3 times the relative standard deviation (s_r) of the RTP intensity in argon was 0.0005% (5 ppm) oxygen in argon, and the precision at 0.02% oxygen level for five determinations was ±0.2%.

Triplet lifetimes obtained using the Obey-Decay program are shown in Table 1. As expected, the triplet lifetime decreases both in the presence of oxygen and of moisture.

Effect of Moisture on the RTP Background Intensity and on the Response to Oxygen of the Sensing Beads

It is well known that the RTP emission of many compounds adsorbed in filter paper, cellulose, silica, *etc.*, decreases drastically in the presence of moisture. In these cases, traces of water disrupt the hydrogen bonds between the RTP luminophor and the support.[16,17] In order to evaluate the effect of moisture in our system, a humidifier with pure de-ionized water was placed immediately before the detector. For experiments with sensing beads, results showed that 100% humidity in the gas flow stream decreased the RTP emission intensities observed in the absence of oxygen (Ar environments) by 38%. However, it was found that in the presence of moisture, the sensing beads also respond to oxygen and, interestingly, the slopes of the calibration graphs, I_o/I *versus* the square root of the concentration of oxygen, were a little higher for humidified than for dry gases, *e.g.*, linear plots:

$$I_o/I - 1 = -0.17 + 2.57\ (\%\ O_2)^{\frac{1}{2}} \text{ for dry mixtures, and}$$
$$I_o/I - 1 = -0.14 + 2.88\ (\%\ O_2)^{\frac{1}{2}} \text{ for humidified gases}$$

were obtained; the linear regressions were 0.9996 and 0.9998, respectively.

The differences in the slopes could be explained by considering that the water contained in the moisturized gases decreased the degree of fixation of the adsorbed dye to the non-ionic resin. This effect makes the RTP emission of the luminophor more sensitive to quenching by oxygen.

Furthermore, it was observed that the sensing beads also respond to oxygen in liquid media (see Fig. 6), as it was demonstrated using a liquid flow system similar to that described previously.[15] For these experiments an aqueous buffer, 0.1 mol l^{-1} acetic acid–sodium acetate at pH 6, was continuously pumped through the system.

Table 1 Triplet lifetimes of immobilized erythrosin B in different environments

Environment	Lifetime/ms	Correlation
Dry argon	0.404 ± 0.002	0.999
Wet argon	0.357 ± 0.003	0.999
Dry argon + 1.26% O_2	0.185 ± 0.010	0.995
Wet argon + 1.26% O_2	0.167 ± 0.010	0.995

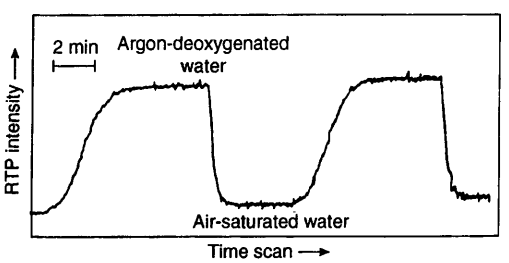

Fig. 6 Response–time curve and reversibility in the response of the sensing beads to oxygen dissolved in aqueous media.

Experiments with Sensing Membranes

The response to oxygen of silicone-sensing membranes prepared under different procedures was evaluated. Fig. 7 shows typical response curves obtained for the gas FI system, using two sensing phases of different thicknesses. The rounded shape of the profiles is indicative of the higher impediments for the oxygen to reach the RTP indicator when sensing membranes are used instead of sensing beads [Fig. 5(*a*)]. Also, as can be seen in Fig. 7, the thicker the membranes the lower the oxygen diffusion processes.

Oxygen detection limits for these membranes were evaluated using the gas FI system and results are collected in Table 2. Table 2 also shows detection limits obtained when using membranes with sensing beads embedded. It can be observed in the latter case that better detection limits are obtained for higher bead density in the silicone membrane.

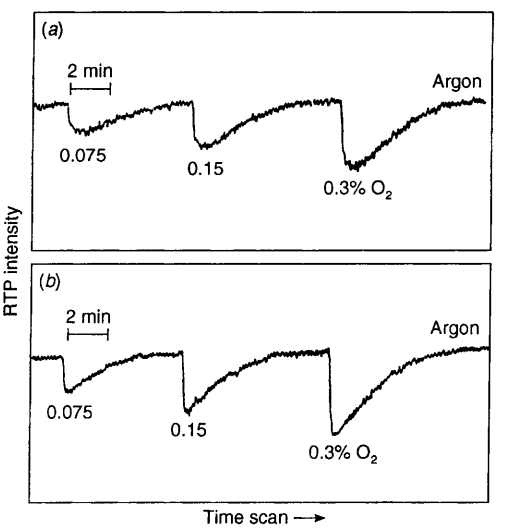

Fig. 7 Response-time signals for the gas FI system using a silicone sensing film of: (*a*) 0.40 mm thickness and (*b*) 0.20 mm thickness.

Table 2 Detection limits and precisions attained for different sensing phases using the gas–FI system

Phase	Detection limits (%)	Precision (%)
Sensing beads (20–60 mesh beads with 3.6×10^{-7} mol adsorbed reagent per gram of XAD-2)	0.0005	±0.3 (at 0.02% O_2)
Sensing films		
(*a*) prepared from a solution of the reagent:		
film 0.20 mm thick	0.0046	±0.4 (at 0.15% O_2)
film 0.40 mm thick	0.0060	±0.4 (at 0.15% O_2)
(*b*) prepared from sensing beads of 200–400 mesh (films of 0.25 mm thickness):		
0.063 g beads per gram of silicone	0.0150	±0.3 (at 0.15% O_2)
0.144 g beads per gram of silicone	0.0085	±0.3 (at 0.15% O_2)

Conclusions

The oxygen sensing phases proposed in the present study offer excellent analytical sensitivities. In fact, the sensing beads prepared by adsorbing Erythrosin B on Amberlite XAD 2 particles give a detection limit for oxygen which is 200 times lower than other RTP sensing phases described for oxygen, which used similar instrumentation.[15] In those studies, negatively charged room-temperature phosphorescent metal chelates were strongly bonded *via* ion-exchange processes to strong anion-exchange resins.[15] A higher degree of immobilization of the indicators bonded by ion-exchange, which make the RTP sensor less susceptible to the presence of quenchers such as oxygen,[1,3] are among the reasons which could account for the lower Stern–Volmer quenching efectiveness observed for the sensing phases with those metal chelates.

These good sensitivities, which could allow the use of minute sensor sizes, along with the long excitation and emission maxima wavelengths (cheap light sources and detectors are available in these regions) open the way for the coupling of the assayed sensing phase to simple instrumentation and to fibre optics for remote oxygen sensing.

Insight into the transduction mechanism of this RTP probe, using triplet lifetime measurements, has also been outlined in studies performed in our laboratory.[20]

The financial support from Fondo de Investigaciones de la Seguridad Social (FISss) Project Ref. 93/0469 is gratefully acknowledged and Dr. A. Sanz-Medel is thanked for helpful discussions.

References

1 Leiner, M. J. P., *Anal. Chim. Acta*, 1991, **255**, 209.
2 Wolfbeis, O. S., and Leiner, M. J. P., *J. Soc. Photo-Opt. Instrum. Eng.*, 1988, **906**, 42.
3 O. S. Wolfbeis, in *Molecular Luminescence Spectroscopy. Methods and Applications: Part 2*, ed. S. G. Schulman, John Wiley, New York, 1988, ch. 3.
4 Peterson, J. I., Fitzgerald, R. V., and Buckhold, D. K., *Anal. Chem.*, 1984, **56**, 62.
5 Optiz, N., Graf, H. J., and Luebbers, D. W., *Sens. Actuators*, 1988, **13**, 159.
6 Wolfbeis, O. S., Weis, L. J., Leiner, M. J. P., and Ziegler, W. E., *Anal. Chem.*, 1988, **60**, 2028.
7 Lippitsch, M. E., Pusterhofer, J., Leiner, M. J. P., and Wolfbeis, O. S., *Anal. Chim. Acta*, 1988, **205**, 1.
8 Sacksteder, L., Demas, J. N., and DeGraff, B. A., *Anal. Chem.*, 1993, **65**, 3480.
9 Li, X. M., Ruan, F. Ch., and Wong, K. Y., *Analyst*, 1993, **118**, 289.
10 Kautsky, H., *Trans. Faraday Soc.*, 1939, **35**, 216.
11 Lee, E. D., Werner, T. C., and Seitz, W. R., *Anal. Chem.*, 1987, **59**, 279.
12 Papkovsky, D. B., *Sens. Actuators, B*, 1993, **11**, 293.
13 Gewehr, P. M., and Delpy, D. T., *Med. Biol. Eng. Comput.*, 1993, **1**, 11.
14 Li, X. M., and Wong, K. Y., *Anal. Chim. Acta*, 1992, **262**, 27.
15 Liu, Y. M., Pereiro-García, R., Valencia-González, M. J., Diaz-García, M. E., and Sanz-Medel, A., *Anal. Chem.*, in the press.
16 Hurtubise, R. J., *Phosphorimetry. Theory, Instrumentation and Applications*, VCH Publishers, New York, 1990, ch. 6.
17 Vo-Dinh, T., *Room Temperature Phosphorimetry for Chemical Analysis*, ed. Elving, P. J., Winefordner, J. D., and Kolthoff, I. M., Wiley, New York, 1984, ch. 4.
18 Lovelock, J. E., *Anal. Chem.*, 1961, **33**, 162.
19 Diaz Garcia, M. E., and Sanz-Medel, A., *Anal. Chem.*, 1986, **58**, 1936.
20 Velasco-García, N., Pereiro García, R., and Diaz-García, M. E., *Spectrochim. Acta Part A*, submitted.

Paper 4/01821D
Received March 28, 1994
Accepted June 28, 1994